Imperial College Press
www.icpress.co.uk

Impact Damage Detection in Composite Plates using a Self-diagnostic Electro-Mechanical Impedance-based Structural Health Monitoring System

Z. Sharif-Khodaei[*], M. Ghajari[†] and M. H. Aliabadi[‡]

Department of Aeronautics, Imperial College London
South Kensington Campus, Exhibition Road, SW7 2AZ, London, UK
[*]z.sharif-khodaei@imperial.ac.uk
[†]m.ghajari@imperial.ac.uk
[‡]m.h.aliabadi@imperial.ac.uk

In this work, application of the electro-mechanical impedance (EMI) method in structural health monitoring as a damage detection technique has been investigated. A damage metric based on the real and imaginary parts of the impedance measures is introduced. Numerical and experimental tests are carried out to investigate the applicability of the method for various types of damage, such as debonding between the transducers and the plate, faulty sensors and impact damage in composite plates. The effect of several parameters, such as environmental effects, frequency sweep, severity of damage, location of damage, etc., on the damage metric has been reported.

Keywords: Impact; structural health monitoring; finite elements; artificial neural network.

1. Introduction

In recent years, the structural health monitoring techniques have been the topic of many research studies. They have received increasing attention due to their capabilities as a nondestructive evaluation (NDE) technique for monitoring a wide range of structures and engineering systems. In particular, their applicability for barely visible damage (BVID) detection caused by an impact event in aircraft composite panels is being assessed. The aim of implementing an SHM system in a structure is to move from schedule-driven inspection to condition-based maintenance, resulting in higher safety and reduction in life-cycle costs.

---

[*]Corresponding author.

Smart structures have integrated sensors and actuators to continuously monitor the state of the structure. Transducers made from lead zirconate titanate (PZT) piezoelectric ceramic patches can be used as both sensors and actuators due to their direct and converse piezoelectric properties simultaneously. PZT patches are light, small and do not require high power and can be surface mounted or imbedded in the structure. PZT patches are used in both passive and active sensing. Passive sensing technique utilizes the PZT transducers as sensors only and can result in impact detection[29,21] and characterization.[4,26,32] Active sensing is comprised of actuating and sensing a network of transducers in turn to detect, localize and characterize damage.[25,24,18,22] Often platforms can be designed having both capabilities of active and passing sensing.[23] The question of the reliability of any SHM system is closely linked with the network architecture, i.e., what is the minimum number of sensors to be able to detect an impact even or the subsequent damage. Optimization algorithms result in the best sensor number and location to reach a required probability of detection with a certain reliability.[16,27]

The electro-mechanical impedance (EMI) method is an attractive active sensing technique. In this method, the actuation and sensing are carried out with one PZT transducer, in contrast to the ultrasonic guided wave methods, which normally require separate actuators and sensors.[20] The fundamental aspect of the EMI active technique is the energy transferred between the transducer and the substrate. Due to the converse piezoelectric effect, a mechanical strain is generated in the transducer by applying a harmonic voltage. The strain is consequently transmitted to the structure. The EMI, which is the ratio between the applied voltage and the current measured at transducer's terminals, is directly related to the mechanical impedance of the structure due to the mechanical coupling between the sensor and the host structure. Hence, the EMI is affected by the presence of any structural damage.

The energy transfer in electro-mechanical systems was first investigated by Liang *et al.*[12] They presented a coupled analysis using a simple PZT actuator model, with one-degree of freedom, and a lumped parameter system in order to study power consumption and energy flow in the system. This model was later extended[33] to model the electro-mechanical behavior of two-dimensional (2D) PZT patches coupled to a 2D host structure. The energy transfer in electro-mechanical systems was later exploited by other researchers to detect damage in structures. Chaudhry *et al.*[3] compared the high frequency EMI signatures of an aircraft structure in healthy (pristine) and damaged conditions. They found that at high frequencies (100–150 kHz), very minor alterations in the structure were detectable and the detection area was limited to the immediate neighborhood of the PZT transducer. A review of the early applications of the EMI method can be found in Ref. 6. The EMI technique was used by Giurgiutiu and Zagrai[7] to detect damage in metallic structures, including thin-skin aircraft panels, and for self-diagnosis of PZT transducers.

Lopes *et al.*[15] applied the EMI method to detect damage in a bridge and a truss structure. The damage was introduced through loosening connecting bolts at

different locations. For the bridge, a frequency range from 21 kHz to 23 kHz was selected and for the truss structure, the frequency was varied between 90 kHz and 105 kHz. Sensors near the damage clearly detected it, but the severity of damage was evaluated through establishing artificial neural networks.

In order to find a damage identification metric suitable for the EMI method, Guirgiutiu *et al.*[9] studied circular aluminum plates (100 mm diameter) with cracks generated at different distances from the center of the plate where the PZT sensor was affixed. The excitations were applied within three frequency bands, namely 10–40 kHz, 10–150 kHz and 300–450 kHz. In the 300–450 kHz band, there was a clear relation between the crack/sensor distance and the third power of the correlation coefficient deviation, $(1 - R^2)^3$; as the distance between the crack and the sensor increased, the damage metric decreased.

In a study on damage detection in concrete beams,[28] the EMI method was employed. The sensors bonded to the beams were excited at frequencies in the range 10–200 kHz, high enough to detect any incipient damage in the concrete. The root mean square deviation (RMSD), calculated with the impedance spectra of the damage and pristine states, was used as the damage metric. The RMSD was measurable (0.6%) for the largest distance (300 mm) between the crack and the sensor. The RMSD continuously increased as the damage progressed toward the sensor. For the FE analysis of the same problem, instead of applying voltage to the sensor, a pair of self-equilibrating harmonic forces was applied to the specimen at the edges of the sensor. The numerical results also suggested that the RMSD can be used as an indicator of the distance of the damage from the sensor.

Park *et al.*[17] studied damage detection in a rail road track by using a combination of the EMI method, with a 40–50 kHz frequency range, and the guided-wave (using the Lamb waves) method. The damage was detected when the damage indicators of these methods were plotted versus each other in a 2D space. A combination of these methods was also proposed by Yu and Giurgiutiu[30] for identification of corrosion in metallic thin-wall structures.

Bhalla and Soh[2] proposed a new method to monitor the health of a structure based on the EMI method. The method was based on characterizing an equivalent lump parameter model for the structure by comparing the conductance and susceptance (real and imaginary parts of the inverse of the impedance, called admittance, respectively) spectra. Damage was identified by comparing the damping constant and stiffness of the lumped parameter model equivalent to the pristine state to those of the model equivalent to the damaged state. These authors also proposed[1] a simplified model for the EMI response of surface bonded structures, which was based on the concept of effective mechanical impedance. They also proposed a method to determine the effective mechanical impedance from the admittance signatures of bonded PZTs.

Liu and Giurgiutiu[11] extracted the impedance spectrum of a free PZT transducer using the FE method and compared the real part of the impedance with experimentally obtained data. In high frequencies (over 1000 kHz), there was a shift

in the resonance frequencies, which was attributed to the mesh size (the element length was 0.25 mm) and the time step of the harmonic analysis. By using a simple FE model of a beam with a surface bonded PZT patch and comparing its numerical impedance spectrum with experimental data, they found that using coupled filed elements excited with voltage, rather than applying forces and moments to simplify the numerical modeling, significantly improves the numerical predictions. Among a few other FE studies of the EMI of structures is the modeling of a glass fiber reinforced polymer beam with a surface bonded PZT transducer by Gresil *et al.*[11] The introduced damage was delamination (0.1 mm to 1 mm long) and material degradation ($0.5 \times 0.5 \, \text{mm}^2$) represented by stiffness reduction. Since the damage size was small, they could be detected with very high frequencies, e.g., 600–800 kHz. The study showed that the RMSD decreased as the distance between the transducer and the damage increased. In addition, the performance of 2D plane-strain elements was comparable to the performance of three-dimensional (3D) solid elements, which are computationally expensive. In a recent computational study,[13] the effects of the damping of the structure and the stiffness of the transducer/structure interface were investigated through predicting the EMI spectrum of an aluminum plate with the coupled field FEM. In a more recent study, Gonsalez *et al.*[10] applied the EMI method for damage detection (loose bolt) in a metallic fuselage panel.

This brief review shows that the EMI technique, due to the high-frequency excitations, can be used for near-field damage identification by placing PZT transducers near critical structural locations. The EMI signature is not sensitive to changes in boundary conditions far from the transducer and to low-frequency vibrations, such as operational vibrations. The change in the real part of the EMI spectrum can be correlated with the distance of the damage from the sensor, while the imaginary part can confirm the integrity of the sensor and its attachment to the structure. However, most of the published research have been carried out on metals or concrete. Very few have investigated the applicability of the EMI method for damage detection in composite structures, in particular BVID caused by impacts in composite structures.

This paper focuses on the applicability of the EMI method for an SHM system applied to composite structures. The EMI method can be used in two different concepts: to increase the reliability of the SHM system and reduce the false alarm by adding self-diagnostic properties to the sensorized system, and by adding damage detection capabilities. The effectiveness of both concepts is investigated in this paper. Section 2 presents the theoretical background behind the EMI technique and how it can be applied to damage detection. Section 3 presents the numerical modeling technique together with some results for detecting debonding between the sensor and the plate. The results from the numerical study are then validated by experimental results for detecting damage in the sensor and in the structure in Sec. 4. Section 5 contains results of the EMI technique applied to a stiffened panel using numerical modeling followed by discussion and conclusion in Sec. 6.

2. Damage Detection using EMI Technique

The EMI technique can be used in assessing the local dynamics of a structure due to the mechanical coupling between the sensor and the host structure. This coupling, through the electro-mechanical coupling inside the PZT sensor, is reflected in the electrical impedance measured at the terminals of the sensor. When a discontinuity or damage is present in a close vicinity to the sensor, the coupling is affected and will change the EMI measures. By comparing the current state of the structure to a baseline signal corresponding to its pristine state, damage can be detected and characterized.

The coupling between the electrical variables (electric field E_k and electrical displacement D_j) and mechanical degrees of freedom (strain S_{ij} and stress T_{kl}) of PZT elements are defined through the general constitutive equation as[5]

$$
\begin{aligned}
D_j &= d_{jkl}T_{kl} + \varepsilon_{jk}^T E_k, \\
S_{ij} &= s_{ijkl}^E T_{kl} + d_{kij}E_k,
\end{aligned}
\tag{1}
$$

where d_{kij} is the piezoelectric constant, ε_{ij}^T is the dielectric permittivity measured at zero stress and s_{km}^E is the compliance of the material measured at zero electric field.

To measure the EMI response, harmonic voltage is applied to the terminals of the PZT. The amplitude of the current propagating through the surface is $I = j\omega Q$, where I is the current, j is the imaginary unit and ω is the excitation frequency. The electro-mechanical admittance is defined as the ratio between the current and the excitation voltage: $Y = I/V$. The impedance is the inverse of the admittance $Z = Y^{-1}$. The complex electro-mechanical admittance is expressed as

$$
Y = \frac{\omega(\text{Re}Q\text{Im}V - \text{Im}Q\text{Re}V)}{\text{Re}V^2 + \text{Im}V^2} + j\frac{\omega(\text{Re}Q\text{Re}V + \text{Im}Q\text{Im}V)}{\text{Re}V^2 + \text{Im}V^2},
\tag{2}
$$

where ω is the excitation frequency. The real part of the admittance is called conductance and the imaginary part is termed susceptance. The impedance is the inverse of the admittance, which can be written as

$$
Z = \frac{\text{Re}Y}{\text{Re}Y^2 + \text{Im}Y^2} - j\frac{\text{Im}Y}{\text{Re}Y^2 + \text{Im}Y^2}.
\tag{3}
$$

The difference in the impedance measured in a healthy structure and a faulty one can be used to detect damage in the structure. This difference in EMI spectrum can be related to a damage metric value and a defined threshold in order to flag up the faulty state. In this work, the RMSD measure is used as the damage index:

$$
\text{RMSD} = \sqrt{\frac{\sum_{i=1}^{n}\left(G_i^D - G_i^P\right)^2}{\sum_{i=1}^{n}\left(G_i^P\right)^2}},
\tag{4}
$$

where G_i are the discrete measured parameters and superscripts D and P indicate damaged and pristine states, respectively. The applicability of the EMI method for

self-diagnosis of the SHM system and impact damage detection in composite panels is assessed in the following sections.

3. Coupled Field Numerical Modeling of Sensor Debonding

There are analytical models for measuring the EMI spectrum for simple structures, such as the model of a disk proposed by[31,8] assuming only axi-symmetric deformation. However, for more complex structures, such as aircraft stiffened panels, analytical models are not available. For development purposes, it is of high importance to have a valid numerical model for assessing the methodology and study the influence of different parameters on the accuracy of the result. It is very expensive and time consuming to damage composite plates in different locations with varying severity, hence the need for a valid numerical model arises. Moreover, it is difficult, if not impossible, to generate the same size and severity of damage in two different locations in a test specimen. In addition, the effect of the environmental conditions on the EMI readings is significant. With a valid numerical simulation, the influence of a single parameter on the EMI measure can be investigated separately.

The proposed numerical model has been validated against published results, Fig. 1, as reported in Ref. 19. In this paper, the numerical model has been applied for the analysis of a CFRP composite laminate of size $300 \times 225 \times 5.6\,\text{mm}$ with 24 laminas placed symmetrically about its mid-plane. The plate was meshed using 1 mm shell elements. The piezoelectric transducers were modeled using 3D piezoelectric brick elements with a 1 mm edge length. Four PZT transducers were surface mounted on the plate as shown in Fig. 2. The same plate was tested experimentally as reported in Sec. 4.
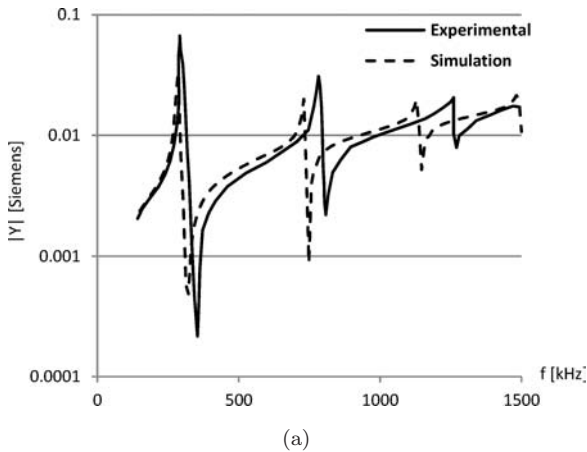

(a)

Fig. 1. Validation of the numerical model against published data (see Ref. 31). (a) Magnitude of admittance signature of free PZT patch as a function of frequency and (b) real part of impedance signature for PZT patch bonded to aluminum disc.
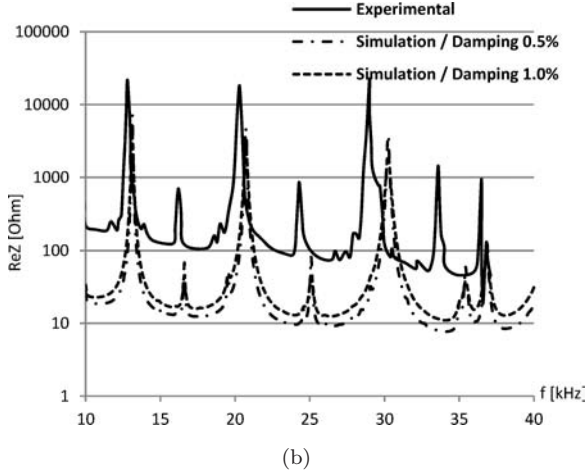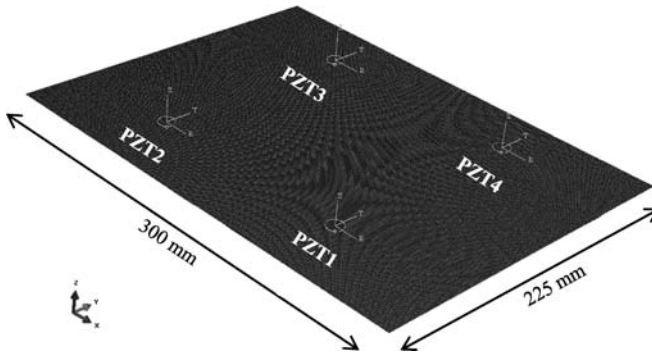
(b)

Fig. 1. (*Continued*)

Fig. 2. CFRP composite panel.

An important factor for the numerical analysis is the damping factor. In this work, structural damping of 5% was added to the plate. Structural damping option assumes that the damping forces are proportional to the forces caused by stressing of the structure and are opposed to the velocity. A linear perturbation simulation with an excitation of $10+j\cdot0\,\text{V}$ sinusoidal voltage sweep from 10–500 kHz across the PZT's terminal was performed using the commercial program ABAQUS. The output from the piezoelectric elements is the charge at the top terminal. A subroutine was developed to extract the frequency and complex reactive charge, calculate the real and imaginary parts of the charge, sum them for all nodes of the top surface set and write the results along with the frequency range.

First, the pristine baselines for all four sensors were taken. Afterward damage was introduced in the form of debonding between PZT1 and the plate in different extents, Fig. 3. Figures 4(a) and 4(b) depict the real parts of the
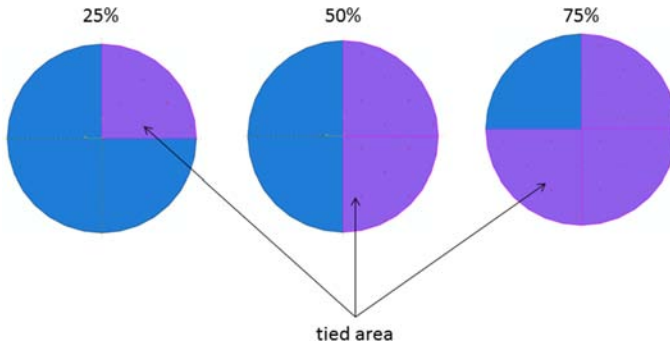
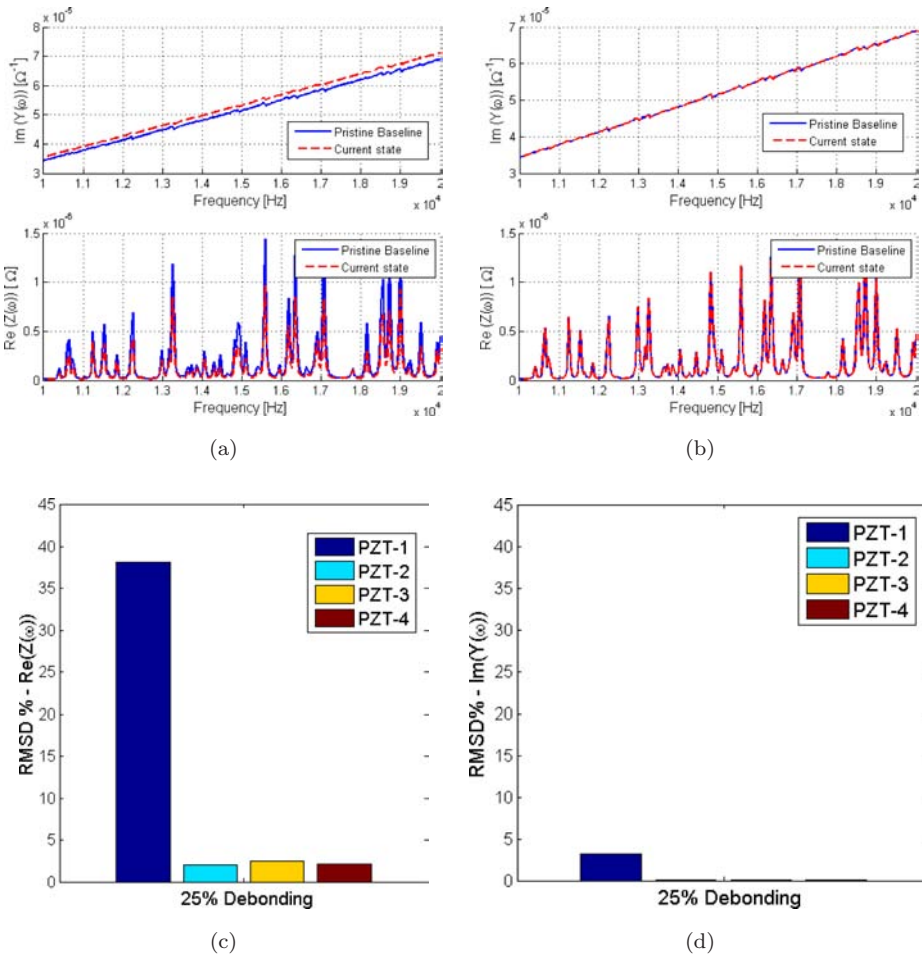Fig. 3. Area of the PZT1 transducer tied to the plate.

(a)　　　　　　　　　　　　　　　(b)

(c)　　　　　　　　　　　　　　　(d)

Fig. 4. EMI measures for PZT1 25% debonded; (a) EMI spectrum in PZT1, (b) EMI spectrum in PZT2, (c) RMSD of Re($Z(\omega)$) and (d) RMSD of Im($Y(\omega)$).
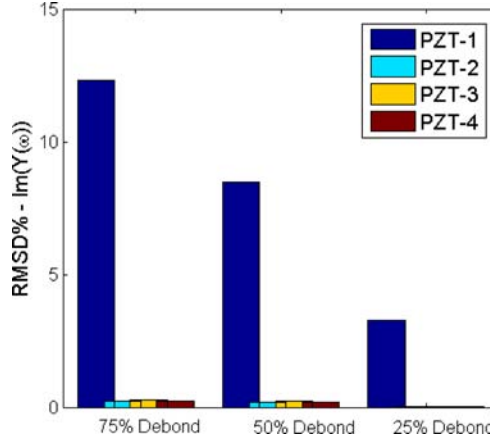
Fig. 5. RMSD% of electrical admittance for different degrees of debonding between PZT1/plate.

electrical impedance, $\text{Re}(Z(\omega))$, and the imaginary part of the electrical admittance, $\text{Im}(Y(\omega))$, spectra in frequency range 10–20 kHz for PZT1 and PZT2, respectively. The damage metric calculated is the RMSD between the baseline curve and the current state (possible damage).

The results in Fig. 4 clearly indicate the presence of damage in PZT1. However, the RMSD values measured from the $\text{Re}(Z)$ show damage values in all transducers, with the highest value at the debonded sensor. Contrary to that, the RMSD measures based on $\text{Im}(Y)$ only flag up damage metric in PZT1. The results for other extents of debonding are shown in Fig. 5.

4. Experimental Verification of the Proposed Methodology

In the previous section, it was shown that using numerical simulation we were able to detect debonding between the sensor and the plate. This section focuses on applicability of the EMI method for damage detection using experimental results taken from composite plates with surface mounted PZT transducers. Two identical CFRP composite plates $300 \times 225 \times 5.6 \, \text{mm}^3$ with symmetric layup have been used in the experimental tests.

The first experiment was to test the repeatability of the measures. EMI measures were taken using an impedance analyzer Wayne Kerr series 6430B for two consequent days to study the influence of environmental effects and test set-up on the baseline measured. The EMI spectra and the RMSD values are plotted in Fig. 6. It shows the importance of defining a threshold value for damage detection to reduce false alarms and to increase reliability of the SHM system. The difference between the RMSD plots of the real impedance and imaginary admittance measures stresses the need for establishing different threshold values for each parameter. However,
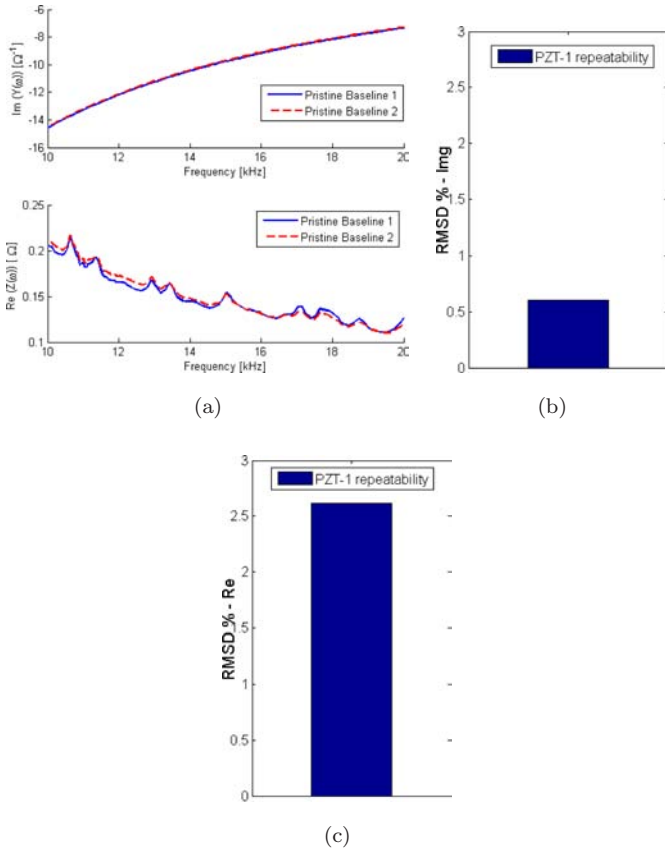
Fig. 6. Environmental effects on the baseline. (a) Frequency plot, (b) RMSD%-Im(Y) and (c) RMSD%-Re(Z).

having two readings is not conclusive to establish a definite threshold and further investigation is proposed for future work.

The second experiment is to study the debonding between the transducer and the plate. Two different severities were tested, namely 50% and 75% debonding. The plots in Fig. 7 show that both ImY and ReZ detect debonding in both sensors. In addition, there is an increase in RMSD value when the debonded area is increased. Both RMSD values are higher than the possible threshold estimated from Fig. 6 ($> 1\%$ for RMSD-ImY and $> 3\%$ for RMSD-ReZ).

The third test was performed to detect a faulty transducer, for a transducer with a notch or a partial crack. The transducer was first scratched to create a surface damage (Crack 1∼2 mm long, Fig. 8(a)) and in the second step it was extended to a notch crack (Crack 2∼3 mm long and 0.1 mm deep, Fig. 8(b)). The influence of both damage extents is visible in Figs. 8(c)–8(h), where both cracks were detected. However, Fig. 8(e) shows the RMSD of ImY for Crack 1 and the level is not very
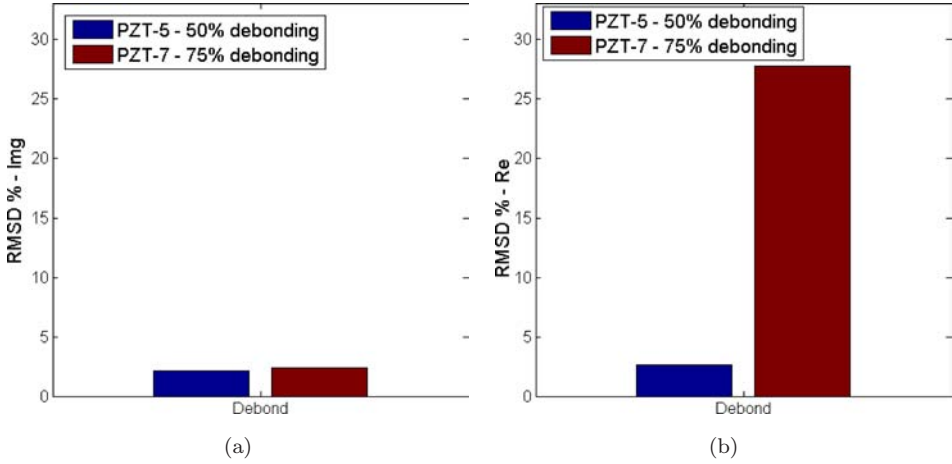
Fig. 7. RMSD values for 50% and 75% debonding. (a) RMSD%-ImY and (b) RMSD%-ReZ.

high; it is around the threshold value of $\sim 1\%$. However, the RMSD of ReZ is above the threshold for both cracks.

The above experiments were carried out to assess the capabilities of EMI method for self-diagnosis of the PZT-based SHM systems. The next step will be to evaluate the competence of the technique in detecting BVID damage in composites.

Two CFRP composite plates $300 \times 225 \times 5.6\,\text{mm}^3$ with symmetric layup were impacted to create BVID. The level of impact energy was kept low in order to cause BVID only. The delamination threshold was estimated according to Eq. (9) defined in Ref. 4 and an impact energy 10% higher than the threshold was chosen. The impact was carried out using a drop tower INSTRON CEAST 9350 machine using a hemispherical impactor with a 2.41 kg mass and 20 mm diameter, see Fig. 9.

Figure 10(a) shows the geometry of the first impacted plate with the impact locations. After each impact, C-scan image of the plate was taken to check if the plate was damaged and to determine the extent and severity of damage. The first plate was impacted with 14.763 J energy, which resulted in a damage area of $\sim 17 \times 18\,\text{mm}^2$, in two different locations. Both impacts resulted in a similar damage extent, shown in Fig. 10(c). The aim was to compare the EMI measures for sensors closer to both damage and observe if there is a trend in the EMI measures. The results for plate P1, after both impacts, are shown in Figs. 11(a)–11(d) for four corner transducers. It was expected to see higher values of RMSD in PZT1 which is closer to both damages in comparison to PZT5. However, the RMSD of ImY (Fig. 11(e)) did not detect damage in PZT1 (value is below the threshold) and the highest value is detected in PZT7. In contrast, the RMSD of ReZ has the highest value in PZT3 (Fig. 11(f)) and still could not detect damage in PZT1 due to low level of damage metric.
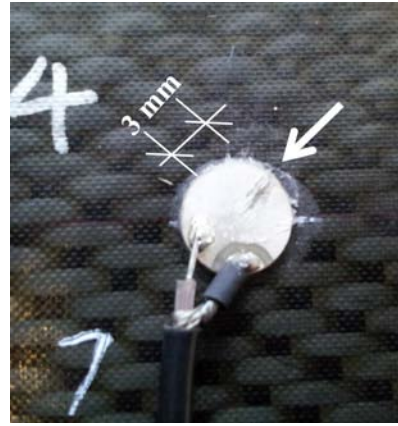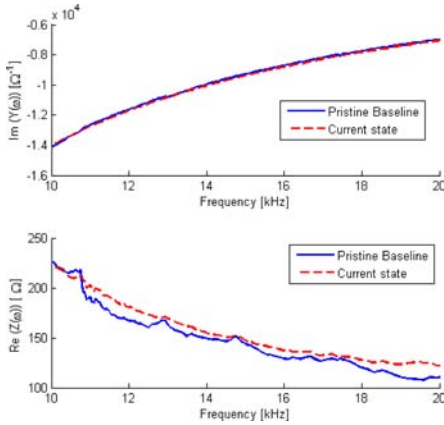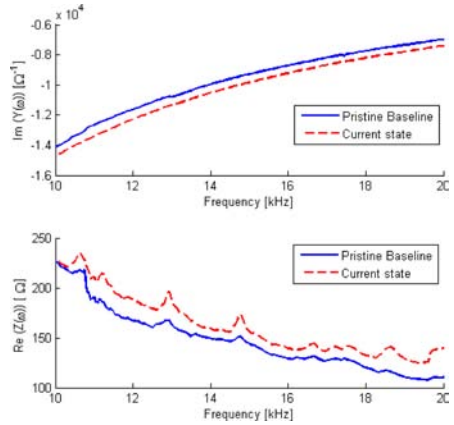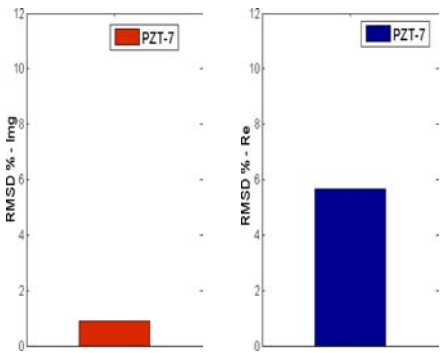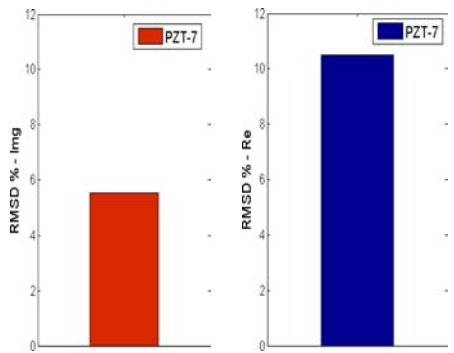
Fig. 8. Detecting a defective PZT. (a) Crack 1, (b) Crack 2, (c) ReZ & Im-Y spectrum for crack 1, (d) ReZ & Im-Y spectrum for crack 2, (e) DI based on ImY-Crack 1, (f) DI based on ReZ-crack 1, (g) DI based on ImY-crack 2, (h) DI based on ReZ-crack 2.
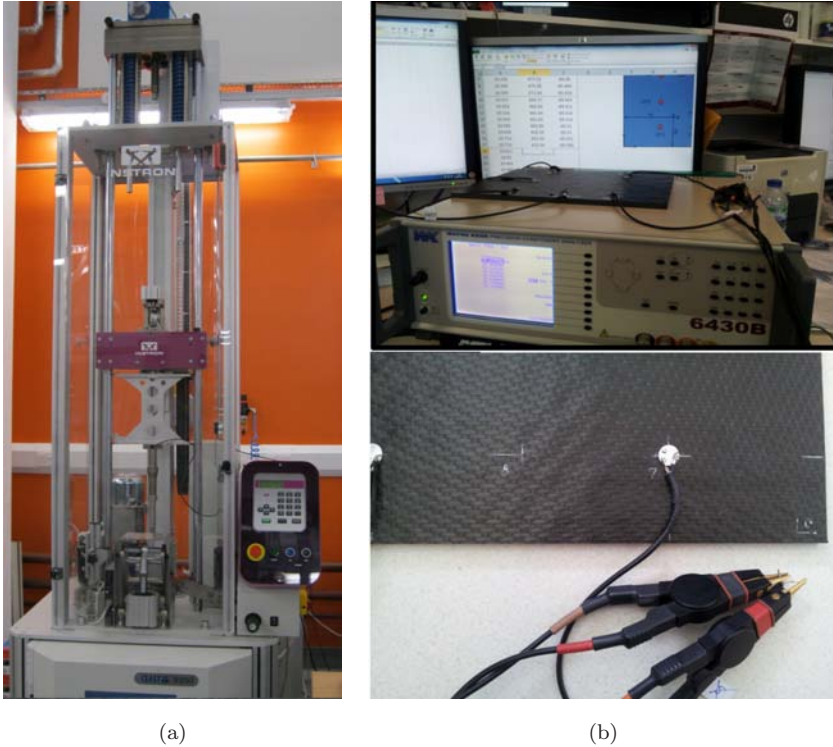
(a)   (b)

Fig. 9. Experimental set-up. (a) Impact tower and (b) Impedance analyzer.

One reason for this mismatch could be that because of the symmetry of the problem, the pristine values were taken only in PZT5 and PZT7 and used for PZT3 and PZT1, respectively. However it seems that the EMI measures are very sensitive to environmental and test set-up conditions and factors such as quality of the bond could play an important role on the baseline. Moreover, the sampling frequency of the impedance analyzer is quite low; therefore, some of the resonance peaks could be missed in the current resolution, especially for higher frequency bands.

Plate 2 was impacted in two steps and after each impact the EMI measures for all the PZTs were taken. Moreover, two different levels of impact energy were chosen to create different damage extents (Figs. 12(c) and 12(d) show the local C-scan images of the impacted areas) to study the influence of damage extent on the EMI measured in the sensors.

The first parameter to investigate was the effect of the frequency band. Ideally, frequencies which contain a large amount of peaks corresponding to the resonance frequencies should be chosen. This is due to the fact that presence of damage in the structure will shift the resonance frequencies or create new ones, therefore the best way to choose the appropriate frequency band is to try different ones and see where
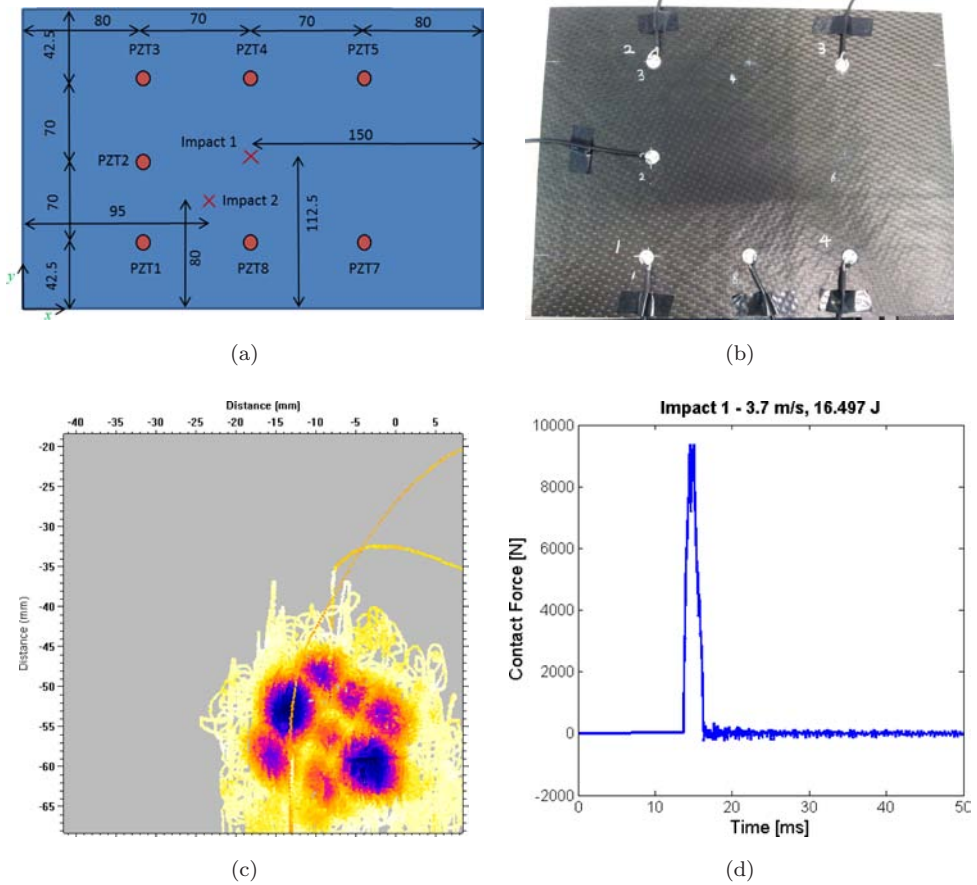
(a)

(b)

(c)

(d)

Fig. 10. Impact test — plate P1. (a) Geometry of transducer and impact locations — plate P1, (b) Composite panel impacted to damage in two locations — plate P1, (c) C-scan image of impact $1 \sim 400 \, \text{mm}^2$ damage and (d) Example of the contact force — impact 1.

the most number of peaks appear. Unfortunately, the resolution of our impedance analyzer was not high enough to study higher frequencies.

Figure 13 shows the results obtained in PZT1, after the first impact in plate P2, for two different frequency bands 10–100 kHz and 10–20 kHz. It is observed that the RMSD values for the frequency band 10–100 kHz is slightly higher in detecting the damage due to Impact 1 in the composite plate. For both frequency bands, damage was successfully detected. Therefore, it is important for every structure to find the appropriate frequency sweep to optimize its response.

Plate P2 was impacted for the second time to create a smaller size of damage. Having the second damage reduces the stiffness of the plate and therefore the value of the RMSD should increase in the sensors. Figure 14 shows the EMI plots and RMSD values in PZT7 after first and second impacts. A clear increase in both RMSD values corresponding to the ImY and ReZ can be seen. Figure 14(a) shows
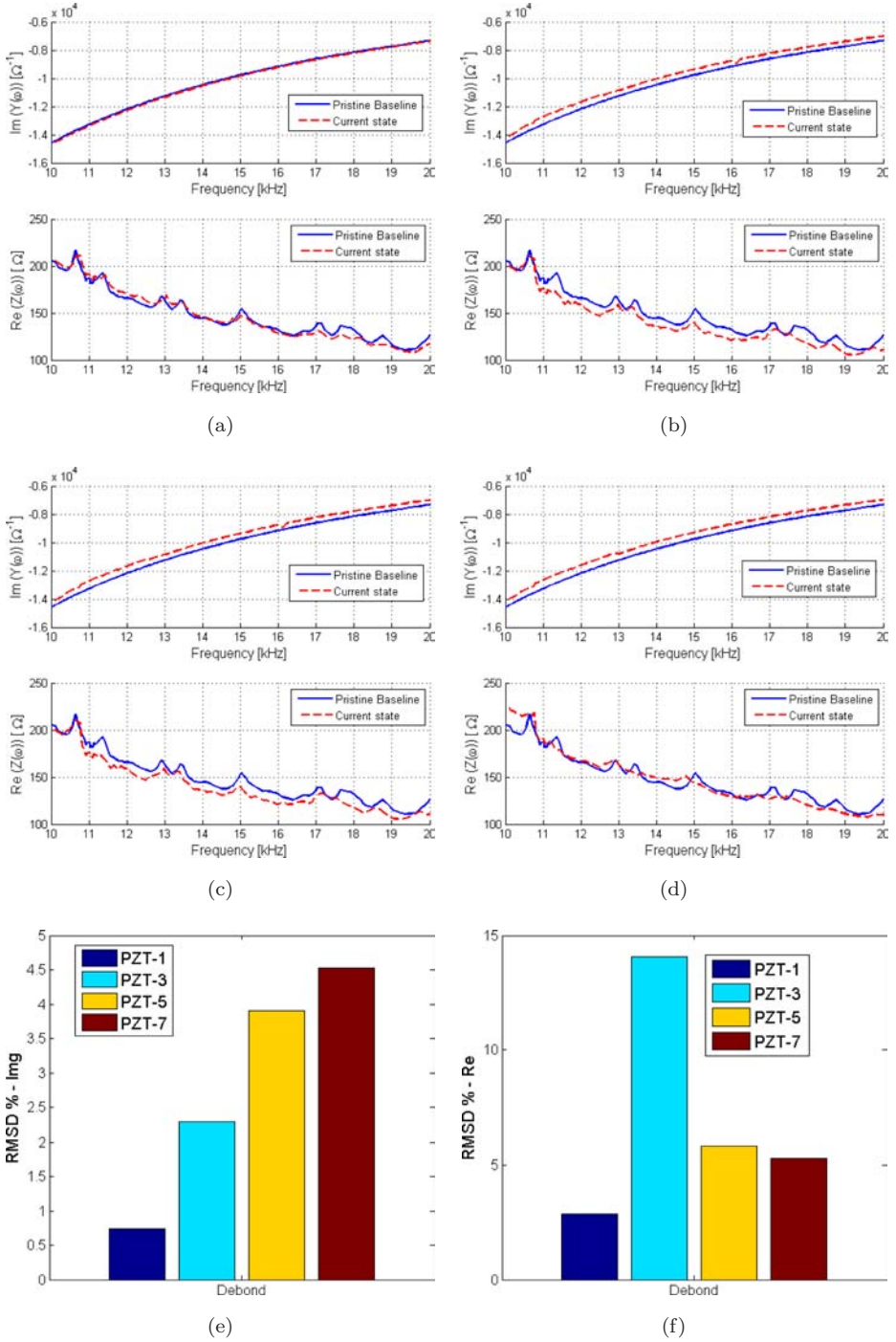
Fig. 11. EMI measures for Plate 1 after two impacts. (a) PZT1, (b) PZT2, (c) PZT 5, (d) PZT 7, (e) ImY and (f) ReZ.
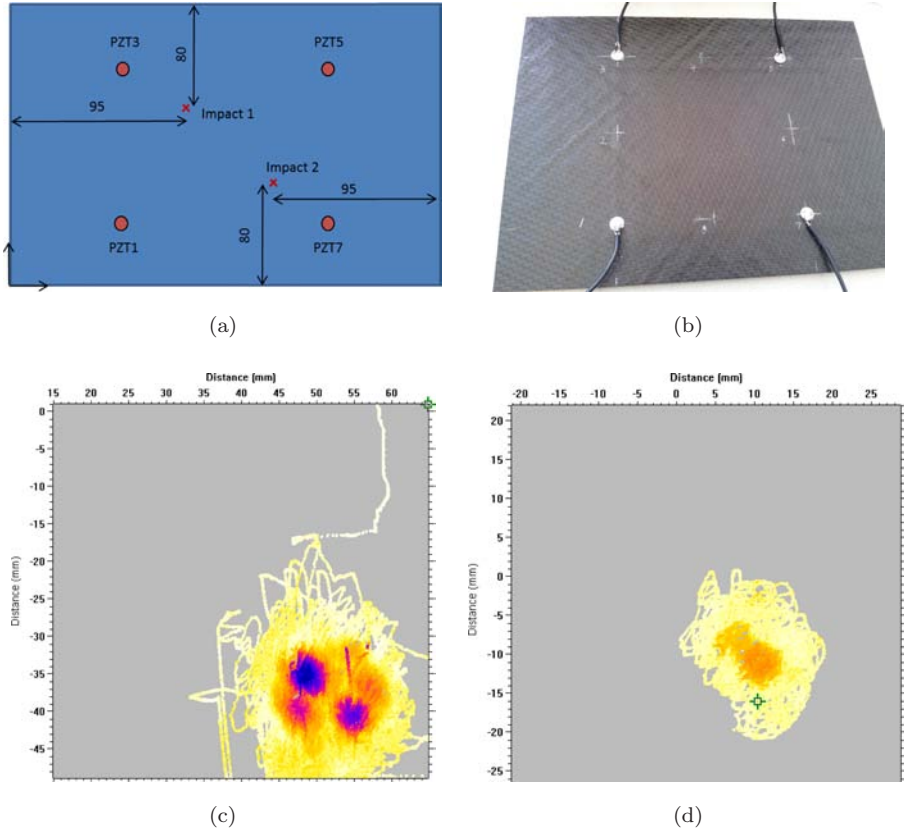
(a)

(b)

(c)

(d)

Fig. 12. Impact test — plate P2. (a) Geometry of transducer and impact locations — plate P2, (b) composite panel impacted to damage in 2 locations — plate P2, (c) C-scan image of Impact 1 location $\sim 200\,\text{mm}^2$ damage and (d) C-scan image of Impact 2 location $\sim 100\,\text{mm}^2$ damage area.
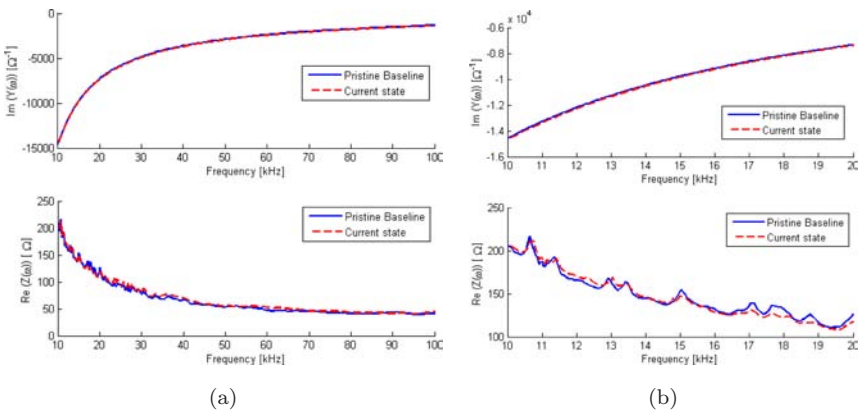

(a)

(b)

Fig. 13. The effect of frequency sweep on the RMSD values for damage detection. (a) Frequency plot 10–100 kHz, (b) frequency plot 10–20 kHz, (c) RMSD% — 10–100 kHz and (d) RMSD 10–20 kHz.

(c)   (d)

Fig. 13. (*Continued*)

(a)   (b)
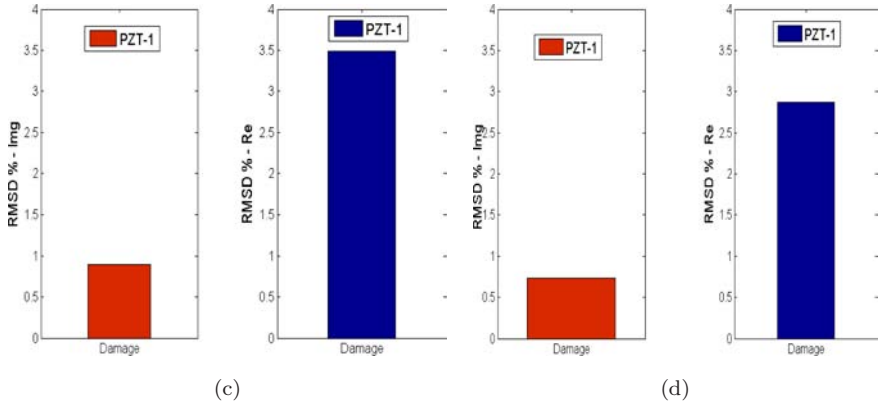

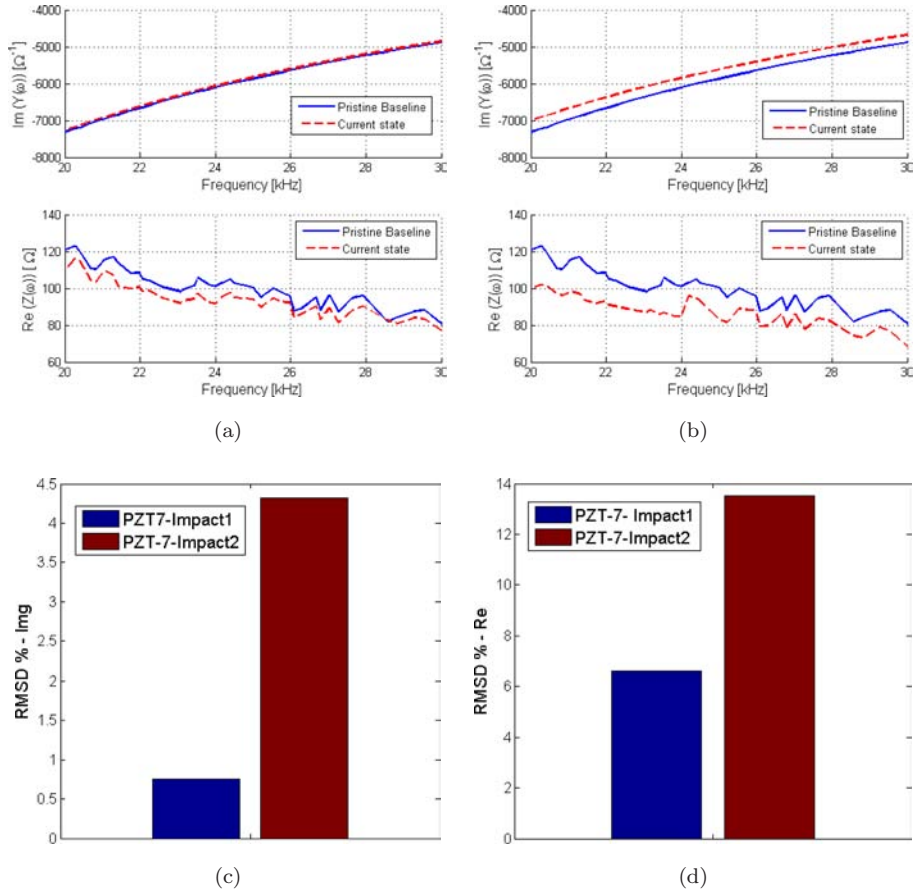(c)   (d)

Fig. 14. Effect of damage extent on EMI measures in PZT 7. (a) EMI frequency plot after Impact 1, (b) EMI frequency plot after Impact 2, (c) RMSD% — ImY and (d) RMSD% — ReZ.

that the ImY after Impact 1 has not changed significantly since the RMSD value is only slightly above the defined threshold. However, the real part of the impedance successfully detected impact damage in both cases.

To examine the influence of damage distance from the sensors, the EMI values in all four sensors were studied as depicted in Fig. 15. If the RMSD values decrease with moving away from damage, then it would be expected to see smaller values of RMSD in PZT1 and PZT5. However, PZT1 and PZT5 show almost the same values of damage metric according to Figs. 15(e) and 15(f). There are many factors, such as resolution of the impedance analyzer, quality of the bond, reliable baseline
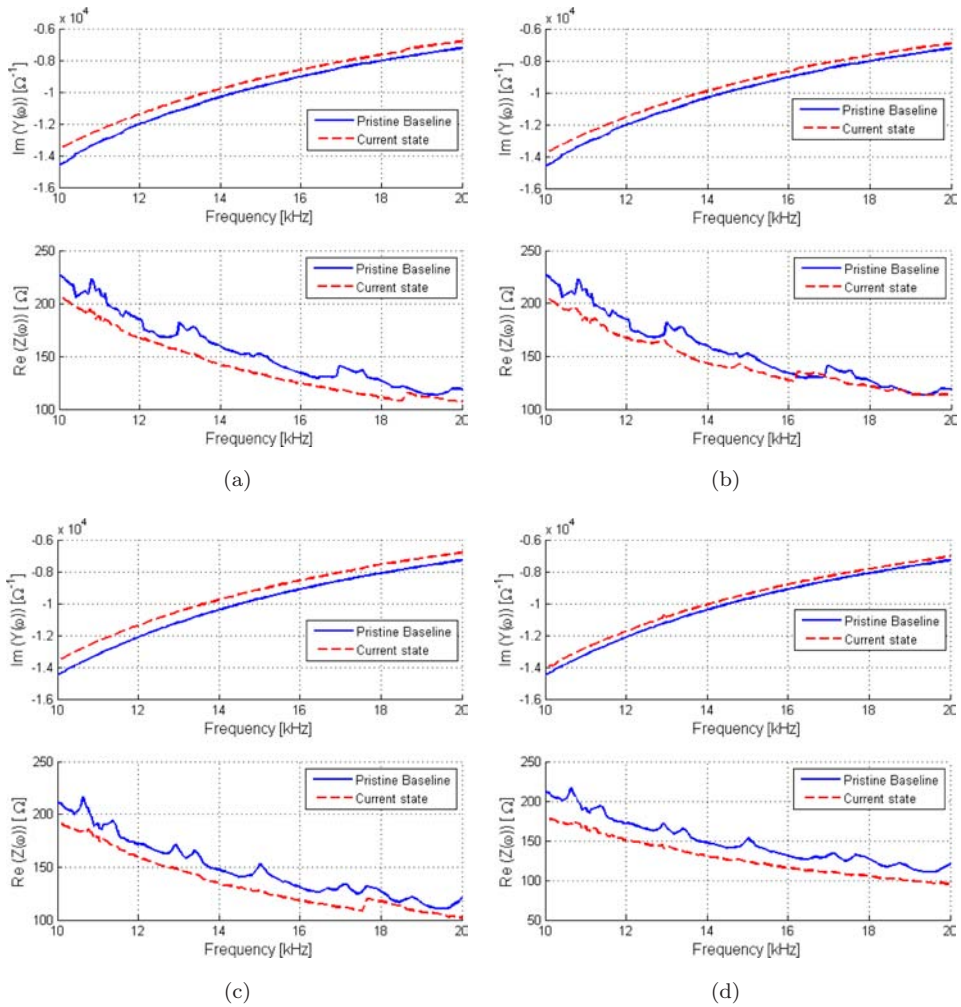

Fig. 15. EMI measures in all four corner sensors after Impact 2 in plate P2. (a) PZT1, (b) PZT3, (c) PZT5, (d) PZT7, (e) ImY and (f) ReZ.
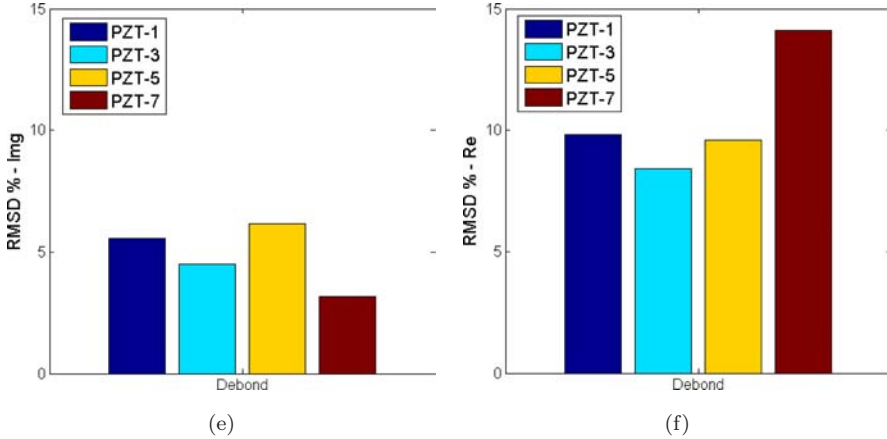
(e)

(f)

Fig. 15. (*Continued*)

signals and environmental effects which can hold us back from making a conclusion on damage characterization using EMI technique. For this reason, a more consistent experiment needs to be carried out to study the effect of each parameter separately. A better experimental set-up with quality control bonding process is proposed for future work to ensure the reliability of the baseline signals. However, from the above experiments, it was clearly shown that EMI method is capable of detecting faulty sensors (self-diagnostic property of the SHM system) and BVID in composite plates.

5. Coupled Field Numerical Modeling of a Composite Stiffened Panel

EMI method was shown to be capable of detecting damage in the structure and in the transducers for self-diagnostics (detecting debonding and crack in the transducer). However, the experimental results were not conclusive for giving any information about the location of the damage. Due to the sensitivity of the baseline measures to environmental conditions (Fig. 6), there is the uncertainty that this could affect the final conclusion. Therefore, a numerical study was carried out to investigate the relation between the damage metric and the location of damage.

A numerical model was developed to simulate debonding between skin and a stringer in part of a composite stiffened panel shown in Fig. 16. It was found that the conductance spectrum of the pristine state in the 20–30 kHz frequency range converges with a shell element size of 1 mm and lower. Therefore, the panel was meshed with 1 mm elements, resulting in approximately 250,000 shell elements. Solving the forced vibration problem at 350 points in the frequency range took 24 h wall-time using eight CPUs and around 50 GB RAM.

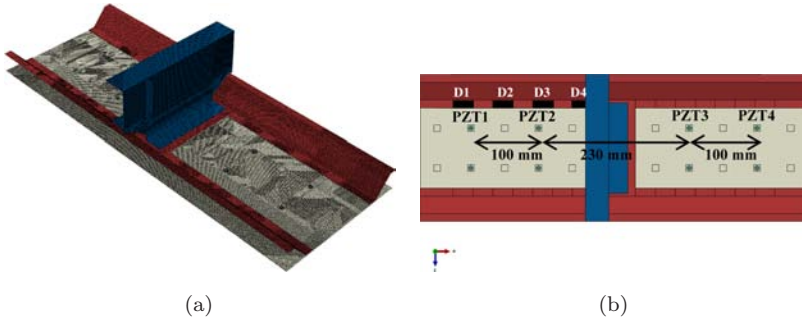<center>(a)   (b)</center>

Fig. 16. FE model of composite stiffened panel with simulated skin/stringer debonding. (a) Stiffened panel — mesh and (b) Geometry for transducers.

Damage was introduced as partial debonding between the stringer and the skin. The length of the debonded area was 30 mm. The damage was then moved in several locations D1, D2, D3 and D4 as shown in Fig. 16(b). The distance between each damage scenario was 60 mm. The EMI measures in four different transducers were compared to see the influence of the location of the damage with regards to each sensor.

The EMI measures for all transducers for debonding D1 is plotted in Fig. 17(a). As can be seen, all transducers detect the damage. There is a definite increase in the damage metric values in PZT1 and PZT2 which are very close to the damage. Transducers PZT3 and PZT4 can detect damage, but they do not provide any further information such as which sensor the damage is closer to. Therefore, it can be established that the RMSD decreases when the distance between the transducer

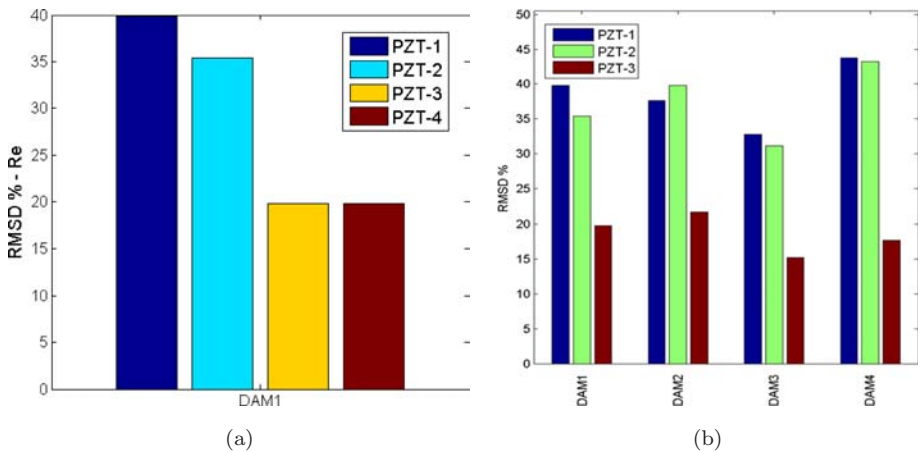<center>(a)   (b)</center>

Fig. 17. RMSD damage metric evaluated for a portion of the stiffened panel. (a) RMSD of ReZ for all sensors due to debonding in D1 and (b) RMSD of ReZ for all sensors for all four debonding locations.

and damage increases. Moreover, Fig. 17(b) shows the damage metric plots for all the transducers and all four debonding locations. There is no monotonic decrease in RMSD values by increasing the distance between the transducers and the damage. In addition, the RMSD reduces significantly when the transducer and the damage are in different bays. Finally, it can be concluded that even though the damage was detected in all cases with all the transducers, no direct relation could be recognized between the location of the damage and the damage metric computed from the EMI measures.

6. Conclusion

In this paper, the EMI method has been assessed as a damage detection technique for SHM systems based on PZT transducers. The applicability of the technique for both self-diagnostic applications and BVID detection was investigated. Both numerical and experimental tests were carried out. Both numerical results and experimental tests showed that debonding between the sensor and plate can be detected with both imaginary part of the admittance and the real part of the impedance. Moreover, the degree of the debonding increased the damage metric. Damage was also detected in a transducer with two different notch sizes. The damage metric was higher when the crack was extended. This is very advantageous in designing a self-diagnostic SHM system to check the quality of the bonds or detect faulty sensors before interrogating the structure for damage detection, which will increase the reliability of the system by reducing the probability of false alarm.

The next part of the paper was dedicated to BVID detection in composite panels. Different degrees of impact damage in several locations were investigated. In all cases, damage was successfully detected. However, it was difficult to establish a direct relation between the location of the damage and the damage metric in different sensors depending on their distance to the damage. Nevertheless, we were able to take the first step in application of the EMI technique to more complicated structures and types of damage, such as BVID in aircraft composite plates.

There are various parameters that can affect the EMI measures, such as the quality of the bond, repeatability of the baseline signals, temperature effect, hardware properties, etc. To be able to establish a reliable relation between the damage metric and damage location, a better controlled experiment needs to be carried out in future works.

References

1. S. Bhalla and C. K. Soh, Structural health monitoring by piezo-impedance transducers I: Modeling, *J. Aerosp. Eng.* **17**(4) (2004) 154–165.
2. S. Bhalla and C. K. Soh, Electro-mechanical impedance technique for structural health monitoring and non-destructive evaluation, in *National Workshop on Structural Health Monitoring, Non-Destructive Evaluation and Retrofitting of Structures.* Indian Institute of Technology Delhi, 2008.

3. Z. A. Chaudhry *et al.*, Local-area health monitoring of aircraft via piezoelectric actuator/sensor patches, in *Smart Structures & Materials' 95* (1995). International Society for Optics and Photonics (1995).

4. M. Ghajari *et al.*, Identification of impact force for smart composite stiffened panels, *Smart Mater. Struct.* **22** (2013) 085014.

5. V. Giurgiutiu, *Structural Health Monitoring: With Piezoelectric Wafer Active Sensors* (Academid Press is an imprint of Elsevier 30 Corporate Drive, Suite 400, Burlington, MA 01803, USA, 525 B street, Suite 1900, San Diego, California 92101-4495, USA, 84 Theobald's Road, London WC1X 8RR, UK).

6. V. Giurgiutiu and C. A. Rogers, Recent advancements in the electromechanical (E/M) impedance method for structural health monitoring and NDE, *5th Annual Intell. Symp. Smart Structures and Materials*, International Society for Optics and Photonics (1998).

7. V. Giurgiutiu and A. Zagrai, Damage detection in simulated aging-aircraft panels using the electro-mechanical impedance technique, *ASME-Publications-AD* **60** (2000) 349–358, Adaptive Structures and Material Systems Symposium, ASME Winter Annual Meeting, Nov. 5–10, 2000, Orlando, FL.

8. V. Giurgiutiu and A. Zagrai, Damage detection in thin plates and aerospace structures with the electro-mechanical impedance method, *Struct. Health Monit.* **4** (2005) 99–118.

9. V. Giurgiutiu *et al.*, Embedded active sensors for in-situ structural health monitoring of thin-wall structures, *Trans. ASME*, *J. Press. Vessel Technol.* **124** (2002) 293–302.

10. C. G. Gonsalez *et al.*, Structural damage detection in an aeronautical panel using analysis of variance, *Mech. Syst. Signal Process.* **52** (2015) 206–216.

11. M. Gresil *et al.*, Predictive modeling of electromechanical impedance spectroscopy for composite materials, *Struct. Health Monit.* **11** (2012) 671–683.

12. C. Liang *et al.*, Coupled electro-mechanical analysis of adaptive material systems—determination of the actuator power consumption and system energy transfer, *J. Intell. Mater. Syst. Struct.* **5** (1994) 12–20.

13. Y. Y. Lim and C. K. Soh, Towards more accurate numerical modeling of impedance based high frequency harmonic vibration, *Smart Mater. Struct.* **23** (2014) 035017.

14. W. Liu and V. Giurgiutiu, Finite element simulation of piezoelectric wafer active sensors for structural health monitoring with coupled-filed elements, *14th Intell. Symp. Smart Structures and Materials & Nondestructive Evaluation and Health Monitoring*, International Society for Optics and Photonics (2007), Proc. SPIE 6529, Sensors and Smart Structures Technologies for Civil, Mechanical, and Aerospace Systems 2007, 65293R (April 10, 2007); doi:10.1117/12.715238.

15. V. Lopes *et al.*, Impedance-based structural health monitoring with artificial neural networks, *J. Intell. Mater. Syst. Struct.* **11** (2000) 206–214.

16. V. Mallardo *et al.*, Optimal sensor positioning for impact localization in smart composite panels, *J. Intell. Mater. Syst. Struct.* **24**(5) (2012) 559–573.

17. S. Park *et al.*, A built-in active sensing system-based structural health monitoring technique using statistical pattern recognition, *J. Mech. Sci. Technol.* **21** (2007) 896–902.

18. M. Radzieński *et al.*, Damage localisation in a stiffened plate structure using a propagating wave, *Mech. Syst. Signal Process.* **39**(1) (2013) 388–395.

19. M. Schwankl *et al.*, Electro-mechanical impedance technique for structural health monitoring of composite panels, *Key Eng. Mater.* **525** (2013) 569–572.

20. Z. Sharif-Khodaei and M. H. Aliabadi, Assessment of delay-and-sum algorithms for damage detection in aluminum and composite plates, *Smart Mater. Struct.* **23**(7) (2014) 075007.

21. Z. Sharif-Khodaei *et al.*, Determination of impact location on composite stiffened panels, *Smart Mater. Struct.* **21** (2012) 105026.
22. Z. Sharif-Khodaei *et al.*, Lamb-wave based technique for multi-site damage detection, *Key Eng. Mater.* **577** (2014) 133-136.
23. Z. Sharif-Khodaei *et al.*, Smart platform for structural health monitoring of sensorised stiffened composite panels, *Key Eng. Mater.* **525–526** (2013) 581–584.
24. Z. Sharif-Khodaei *et al.*, Lamb-wave based technique for impact damage detection in composite stiffened panels, *Key Eng. Mater.* **488** (2012) 5–8.
25. Z. Su *et al.*, Guided lamb waves for identification of damage in composite structures: A review, *J. Sound Vib.* **295** (2006) 753–780.
26. M. Thiene *et al.*, Effects of the transfer function evaluation on the impact force reconstruction with application to composite panels, *Compos. Struct.* **114** (2014) 1–9.
27. M. Thiene *et al.*, Optimal sensor placement for damage detection based on ultrasonic guided wave, *Key Eng. Mater.* **665** (2015) 269–273.
28. K. K. Tseng and L. Wang, Smart piezoelectric transducers for in situ health monitoring of concrete, *Smart Mater. Struct.* **13** (2004) 1017.
29. K. Worden *et al.*, Natural computing for mechanical systems research: A tutorial overview, *Mech. Syst. Signal Process.* **25** (2011) 4–111.
30. L. Yu and V. Giurgiutiu, Multi-mode damage detection methods with piezoelectric wafer active sensors, *J. Intell. Mat. Syst. Struct.* **20** (2009) 1329–1341.
31. A. Zagrai, Piezoelectric-wafer active sensor electro-mechanical impedance structural health monitoring. Ph.D. thesis, University of South Carolina (2002).
32. Y. Zhong *et al.*, Multi-impact source localisation on aircraft composite structure using uniform linear PZT sensors array, *Struct. Infrastruct. Eng.* **11**(3) (2014) 310–320.
33. S. W. Zhou *et al.*, An impedance-based system modeling approach for induced strain actuator-driven structures, *J. Vib. Acoust.* **118** (1996) 323.